


# Biocompatibility of antibacterial Ti–Cu sintered alloy: in vivo bone response

Bing Bai<sup>1</sup>  · Erlin Zhang<sup>2</sup> · Hui Dong<sup>3</sup> · Jie Liu<sup>3,4</sup>

Received: 9 June 2015 / Accepted: 5 October 2015 / Published online: 27 October 2015  
© Springer Science+Business Media New York 2015

**Abstract** Ti–10Cu sintered alloy has shown very strong in vitro and in vivo antibacterial property and in vitro cell compatibility. In this paper, Ti–10Cu implant (Ti–Cu group) and commercial pure Ti implant (cp-Ti group) were implanted in rabbit femurs to investigate in vivo bone response to the Ti–10Cu alloy. X-ray photo, fluorescent microscopy, routine pathological examination and immunohistochemistry have been used to analyze bone growth, mineral apposition rate (MAR), bone implant contact (BIC), BMP-2 expression and TGF- $\beta$ 1 expression. In both Ti–Cu and cp-Ti groups, new bone tissue was found at bone/implant interfaces 4 weeks postimplantation and completely filled the interfaces gap bone 12 weeks postimplantation. A significant MOD value in BMP-2 expression was observed at week 1 and week 4 in the Ti–Cu group with lower values of week 2 and 3 in both groups, which indicated strong positive activity. MOD value in TGF- $\beta$ 1 expression decreased with the extension of

implantation. However, no difference can be found in MAR, BIC and TGF- $\beta$ 1 expression between the two groups at all intervals. It was deduced that Ti–Cu alloy exhibited as good bone response as cp-Ti. The good bone compatibility suggests that Ti–10Cu alloy might have potential application in orthopedic surgery and dental implant.

## 1 Introduction

Devices are the main cause for the clinical infection and inflammation in orthopedic surgeries and dental implants. To reduce such infection and inflammation, systematic antibiotic has been widely used in clinics, which might bring about side effects to patients. Bacteria colonize surgical implant surfaces easily, which may result in infections that cause implantation failure. Serum proteins like to accumulate on the implant surface, promoting bacteria adhesion and colonization [1]. These can form a biofilm which can help bacteria to escape from the immune surveillance or resist antibiotics [2]. Such a film is critical to clinical infection problems [3].

On the other hand, antibacterial materials have been testified to exhibit strong antibacterial property not only on the surface but also in whole materials, such as antibacterial stainless steel [4] and titanium alloys [5–8]. Antibacterial stainless steels have exhibited very good antibacterial property in vitro and in vivo [9, 10]. Experiments with bacterial adhesion on titanium (Ti), titanium nitride (TiN), fluorine modified hydroxyapatite (FHA) and zinc modified FHA (Zn-FHA) thin films have testified that Ti film with native surface oxide layer and Zn-FHA film showed good antibacterial property and their surface roughness had the least influence on *Porphyromonas gingivalis* adhesion [11]. Other researchers have testified that

✉ Bing Bai  
bingbay119@gmail.com

✉ Erlin Zhang  
zhangel@atm.neu.edu.cn

<sup>1</sup> Department of Prosthodontics, School of Stomatology, China Medical University, Shenyang 110001, People's Republic of China

<sup>2</sup> Key Laboratory for Anisotropy and Texture of Materials, Education Ministry of China, Northeastern University, P. O. Box 350, Shenyang 110819, People's Republic of China

<sup>3</sup> Jiamusi University, Jiamusi 154007, People's Republic of China

<sup>4</sup> Department of Prosthodontics, The Affiliated Hospital of Medical College, Qingdao University, Qingdao 266003, People's Republic of China

silver ion could decrease bacterial adhesions, such as *Escherichia coli*, *Pseudomonas aeruginosa*, *Staphylococcus epidermidis*, and *Staphylococcus aureus*, and less biofilm than titanium and stainless steel bare substrates [12]. Zero valent iron nanoparticles ( $\text{Fe}_{\text{zero}}$ -NPs) and iron oxide nanoparticles ( $\text{Fe}_{\text{ox}}$ -NPs), synthesized at the subsurface and surface of titanium oxide coatings (TOCs) by plasma immersion ion implantation, showed selective antibacterial ability which could kill *S. aureus* under dark conditions but had no obvious effect against *E. coli* [13]. A study that investigated the antibacterial activity and cell adhesion of commercially pure titanium (Ti) surfaces modified by zinc plasma immersion ion implantation (Zn-PIII) treatments showed that Zn-PIII-treated Ti surfaces could significantly reduce *P. gingivalis* and that the numbers of bacteria gradually decreased with increasing Zn concentration [14].

Shirai et al. have reported that Ti–Cu alloys had antimicrobial activity and substantially reduced the incidence of pin tract infection in vitro and in vivo [5]. In our previous study, antibacterial titanium alloys (named Ti–Cu alloys) were produced by sintering titanium powder and copper powder at a high temperature [6] and exhibited high antibacterial rate (up to 99.9 %) against *S. aureus* and *E. coli* [7] and moderate antibacterial rate against *P. gingivalis* in vitro (data isn't shown). The antibacterial property of the Ti–Cu sintered alloys depended on the Cu content, which has to be at least 5 wt% [8]. It has been widely accepted that  $\text{Cu}^{2+}$  ion release from antibacterial coatings or materials plays a very important role in antibacterial behavior [15].

Studies covered effect of  $\text{Cu}^{2+}$  ion implantation on the antibacterial activity of metals including 317L of stainless steels, pure titanium and Ti–Al–Nb alloy, implanted with copper ions using a MEVVA source ion implanter with ion doses ranging from  $0.5 \times 10^{17}$  to  $4 \times 10^{17}$  ions/cm<sup>2</sup>. The results indicated that  $\text{Cu}^{2+}$  ion implantation improved the antibacterial effect for all three materials. At low ion doses ( $0.5\text{--}2 \times 10^{17}$  ions/cm<sup>2</sup>), antibacterial effect was relatively low (smaller than 99 %), and the three materials showed strong antibacterial activity after copper ion implantation at  $4 \times 10^{17}$  ions/cm<sup>2</sup> [11]. Libin Zhu has evaluated the antibacterial activity of copper surfaces on copper resistant and sensitive strains of *Salmonella enterica*. The results showed that under dry incubation conditions, *S. enterica* only survived 10–15 min on high-copper-content alloys but showed 3–4 log reductions on low copper content alloys. Under moist incubation conditions, no survivors were detected after 30 min–2 h on high-copper-content alloys, while the cell counts decreased 2–4 logs on low copper content alloys. The antibacterial effect improves with the increase of ion dose in all cases and high

$\text{Cu}^{2+}$  ion concentration normally leads to a high antibacterial rate [16].

Research has proven that Ti–Cu sintered alloys have good cell biocompatibility and antibacterial property in vitro, but could we apply them clinically? To answer this, we should do more experiments. In this paper, Ti–Cu sintered alloys and cp-Ti were implanted into rabbit femurs to investigate their bone-bonding ability. Understanding the osseointegration of Ti–Cu sintered alloys will be helpful for the practical use of the alloys.

## 2 Materials and methods

### 2.1 Samples preparation

High-purity titanium powder (99.99 wt%, 45–60  $\mu\text{m}$ ) and 10 wt% high purity copper powder (99.99 wt%, 20–60  $\mu\text{m}$ ) were ball milled for 3 h, then hot-pressure sintered into ingots (Ti–10Cu) 25 mm in diameter under vacuum with 25 MPa pressure at 1050 °C for 120 min and cooled in furnace down to room temperature [6, 8]. Samples with a diameter of 2.0 mm and a length of 10 mm were cut from the Ti–Cu ingot for further experiments. Samples were also cut from a commercial pure titanium wrought rod (named cp-Ti) with the same dimensions. All samples were ground with SiC paper up to 1200 grits, ultrasonically cleaned in alcohol for 5 min, and dried in warm air. Before implantation, samples were sterilized by autoclaving at 121 °C for 30 min.

### 2.2 Experimental animals and surgical implantation

The Experimental Animals Centre of China Medical University supplied all animals. Healthy rabbits were used in this study after 2 weeks of observation. 24 female and 24 male adult New Zealand white rabbits (authorization number: SYXK LIAO 2003- 0013), which were 6 months old and weighed 2.0–2.5 kg, were used for the animal experiments. Animal experiments were conducted according to ISO 10993–2:1992 animal welfare requirements. The study was performed in the femoral shaft of the 48 rabbits for 1, 2, 3, 4, 8 and 12 weeks, as listed in Table 1.

**Table 1** Number of rabbits for different examinations

Experiments	Postimplantation (weeks)					
	1	2	3	4	8	12
Immunohistochemistry	8	8	8	3		
Fluorescent observation				3	4	4
Pathological examination				2	4	4

Each animal received 4 implants: one Ti–10Cu implant and one cp-Ti implant in each femoral shaft (Fig. 1). To control selective bias, we kept gender and weight distribution consistent in each group through the stratified randomization grouping law, and ensured the two types of implants were properly placed at the same position in each rabbit.

The animals were anaesthetized with intramuscular (i.m.) injections of pentobarbital (30 mg/kg, 3 % TIANWUD<sup>®</sup>, Tianjin, China), supplemented by 2–4 mg/kg every 30 min. Both lower limbs were shaven and disinfected with a tincture of iodine after fixing the animal. Operations were under sterile conditions. A 3–4 cm cutaneous incision was made parallel to the femur and 5 mm away from its edge. The bone was exposed through skin incisions and blunt dissection of the underlying tissue, including the periosteum. Ti–10Cu and Ti implants were implanted into the middle body of the femur after pre-drilling with a 2.0 mm hand-operated drill, interval of 10 mm, as shown in Fig. 1. The operation site was rinsed with saline, and the tissues were sutured in separate layers and finally sterilized. Pentobarbital (30 mg/kg, i.m. b.i.d. for 48 h) was administered for immediate postimplantation installation pain control. The animal was repositioned and given penicillin (80 u/d, TIANWUDR<sup>®</sup>, Tianjin, China) through i.m. injections for 3 days postoperatively to prevent infection. The animal's temperature was monitored and recorded for 10 days.

### 2.3 Animal sacrifice

Twenty-four rabbits were sacrificed through an auricular venous air embolism after each pre-defined study period of 1, 2 and 3 weeks. Another 24 rabbits were sacrificed through an auricular venous air embolism at 4, 8 and

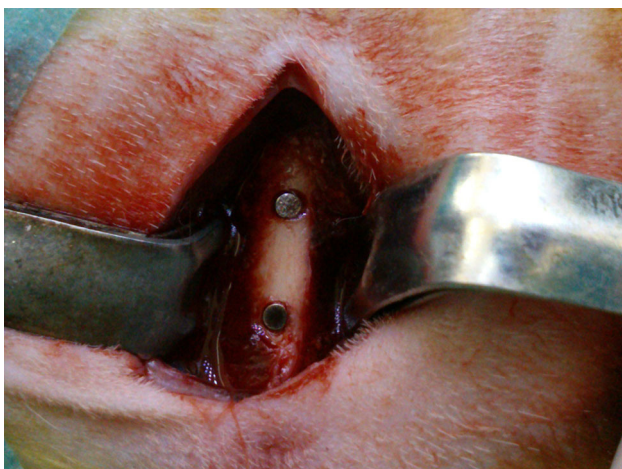


**Fig. 1** Implantation of Ti–10Cu implant and cp-Ti implant for bone response

12 weeks. To investigate the new bone formation process, animals were given calcein (30 mg/100 mL + 2 g Na<sub>2</sub>HPO<sub>4</sub>) (Sinopharm chemical reagent Tianjin Co., Ltd, Tianjin, China) with a dose of 1 mL/kg via muscular injection at 1 and 2 weeks before each sacrifice time.

### 2.4 Fluorescent microscopy

A macroscopic examination of the implanted femur was performed. The implants and the surrounding bone were then removed en bloc. The specimens at each time point were immersed in a 4 % phosphate buffered paraformaldehyde solution for 2 weeks in a refrigerator at a temperature of 4 °C. An X-ray photo observed the bone tissues contacted to the implant.

After flushing with running water for 24 h, the specimens were dehydrated in a series of ethanol rinses (from 70 to 100 %). After dehydration and transparency, the specimens were embedded in a combination of methyl methacrylate and dibutyl phthalate. The tissue blocks were then sectioned using a diamond-saw microtome (EXAKT,

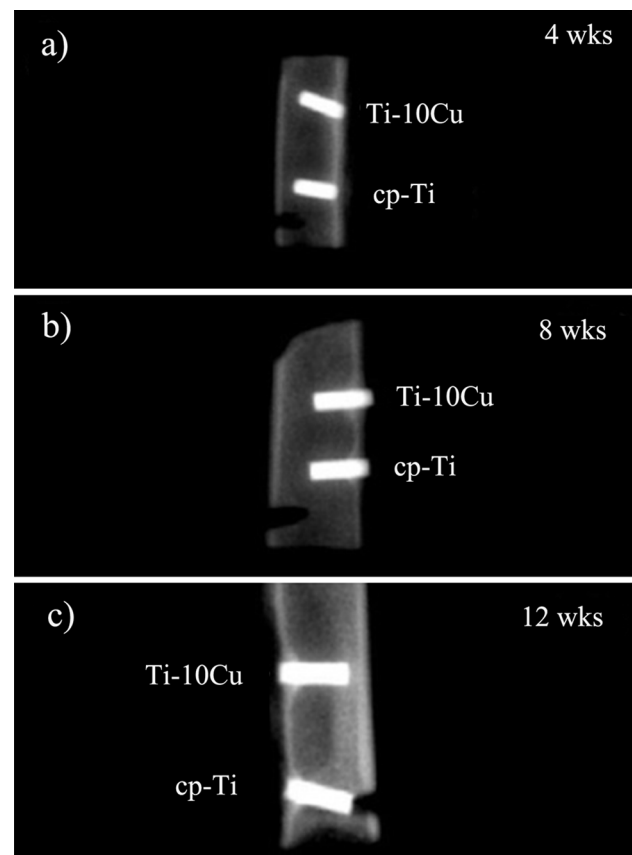


**Fig. 2** X-ray photo of the bone sample with cp-Ti implant and Ti–10Cu sample at different periods postimplantation: **a** 4 weeks, **b** 8 weeks, **c** 12 weeks

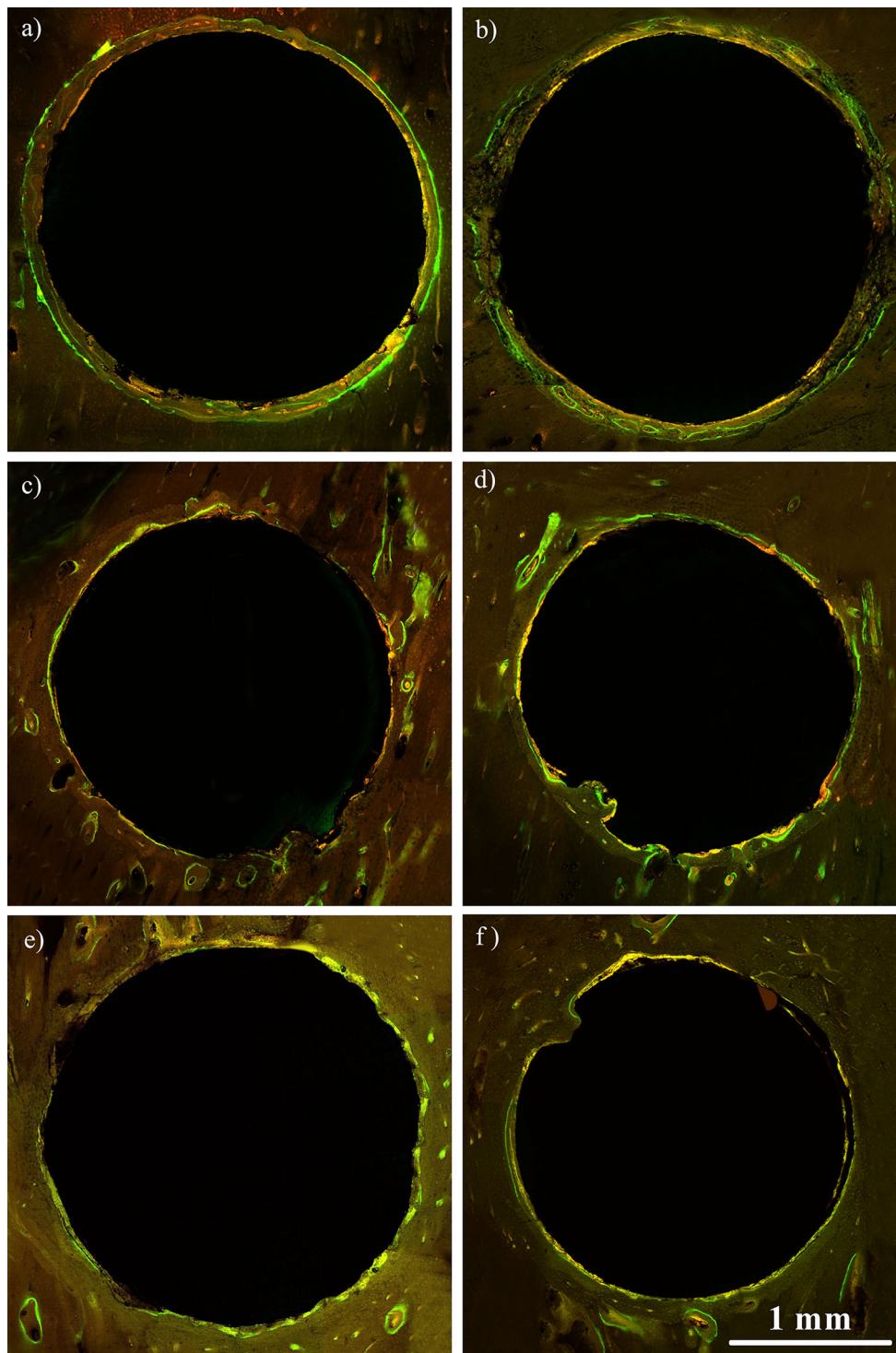


**Fig. 3** Fluoroscopic images of the cross-section of bone specimen with cp-Ti implant and Ti-10Cu implant at different implantation duration ( $\times 40$ ). **a, c** and **e** bone specimen with cp-Ti implant; **b, d** and

**f** bone specimen with Ti-10Cu implant. **a, b** 4 weeks postimplantation, **c, d** 8 weeks postimplantation, **e, f** 12 weeks postimplantation. (The *dark areas* in the *center* are the implants 2 mm in diameter)

E310, Norderstedt, Germany) to obtain 70–80  $\mu\text{m}$  thick sections. The resulting sections were attached to a slide using a resin adhesive. A load of 500 N was applied perpendicular to the sections for 24 h. After the resin adhesive

was completely dried, the samples were subsequently ground to a thickness of 30–40  $\mu\text{m}$  thick by SiC papers up to #2000 and finally polished with emery paste and a cloth wheel (EXAKT, E400CS/AW, Norderstedt, Germany).



Six Ti–10Cu implants and six cp-Ti implants for 4 week, eight Ti–10Cu implants and eight cp-Ti implants for 8 and 12 weeks have been slid into hard-tissue section slices. The hard-tissue section slice, which have the same sequence number, were viewed on a light microscope (Nikon eclipse 80i, Tokyo, Japan) with a heat-barrier, filtered, fluorescent light source (Model C-SHG1, Nikon corp, Tokyo, Japan). Fluorescence microscopic images were taken at 450–480 nm wave lengths. These fluorochromes' colors were clearly distinguishable, and thus could be used sequentially, to highlight the bone neo-deposition, respectively, to each marking period. The dynamic histomorphometric parameter considered was the mineral addition rate (MAR,  $\mu\text{m}/\text{day}$ ), calculated as the distance between the corresponding edges of two consecutive labels divided by the time of the labelling periods, which were measured on the screen by an image analysis software (Image-Pro Plus 6.0, USA). Parameter calibrations for magnification ( $\times 40$ ) and image acquisition were fixed on the basis of standardized conditions imposed before the analysis. For each sample, six sections (from the surface to inside the bone) and four images per section were analyzed.

## 2.5 Immunohistochemistry

For immunohistochemistry examination, the rabbits were sacrificed at 1, 2, 3, and 4 weeks postimplantation, respectively. Bone specimen with Ti–10Cu implant and Ti implant were taken and fixed in 4.0 % formaldehyde solution for 1 week. The bone specimens were decalcified in 15 % EDTA solution until the bone tissue can be easily punctured by pin. There were 8 Ti–10Cu implants and 8 cp-Ti implants for 1, 2 and 3 weeks, 6 Ti–10Cu implants and 6 cp-Ti implants for 4 weeks. Then, implants were taken out from the decalcified bone specimens carefully to damage to the surrounding tissue as little as possible. The bone specimens were embedded in paraffin and cut into 15 thin slices of about 10  $\mu\text{m}$  in thickness by paraffin slicing machine (CUT5062, SLE, Mainz, Germany). Tissue slices, in accordance with the sequence number from the surface to inside the bone, were deparaffinized. Deparaffinized sections were pretreated with 0.3 %  $\text{H}_2\text{O}_2$  for 30 min. After three washings with distilled water, the sections were blocked with a 10 % normal goat serum solution for 40 min at room temperature. BMP-2 antibody (BA2820–1,1:200, Bosterbiological engineering Co., Ltd, Wuhan, China) and TGF- $\beta$ 1 antibody (BA0294, 1:200, Bosterbiological engineering Co., Ltd, Wuhan, China) were applied onto the sections, and maintained at 4  $^\circ\text{C}$  for 48 h in a humid chamber. After three PBS washings the sections were reacted with biotin-goat anti-rabbit IgG (BA1003, 1:200, Bosterbiological engineering Co., Ltd,

Wuhan, China) for 20 min at 37  $^\circ\text{C}$ . After three rinses with PBS, strept avidin–biotin complex (SABC) (SA1022, Bosterbiological engineering Co., Ltd, Wuhan, China) was applied onto the sections, and maintained 30 min at 37  $^\circ\text{C}$ . After three rinses with PBS, visualization of the antibody was accomplished by incubating sections in 0.03 % 3,3'-diaminobenzidine (DAB) (AR1000, Bosterbiological engineering Co., Ltd, Wuhan, China) for 5 min, and the sections were counterstained in hematoxylin. Primary antibody replacement with PBS from the same animal samples was used as the controls. Positive signals were stained brown. Sections were observed on a light microscope (Nikon eclipse 80i, Tokyo, Japan) and assessed quantitatively by calculating the mean optical density (MOD) value at the bone/implant interface using image-analysis software (Image-Pro Plus 6.0, USA). For each specimen and factor, four fields of each section were randomly selected for quantitative assessment. Parameter calibrations for magnification and image acquisition were fixed on the basis of standardized conditions imposed before the analysis.

## 2.6 Masson staining

For Masson staining, the rabbits were sacrificed at 4, 8 and 12 weeks postimplantation, respectively. Samples were deparaffinized and rehydrated through 70, 95 and 100 % alcohol and washed in distilled water, then rinsed by running tap water for 5–10 min to remove the yellow color. After this, the samples were stained in Weigert's iron hematoxylin working solution for 10 min, rinsed in running warm tap water for 10 min and washed in distilled water, and then stained in Biebrich scarlet-acid fuchsin solution for 10–15 min, washed in distilled water and differentiated in phosphomolybdic–phosphotungstic acid

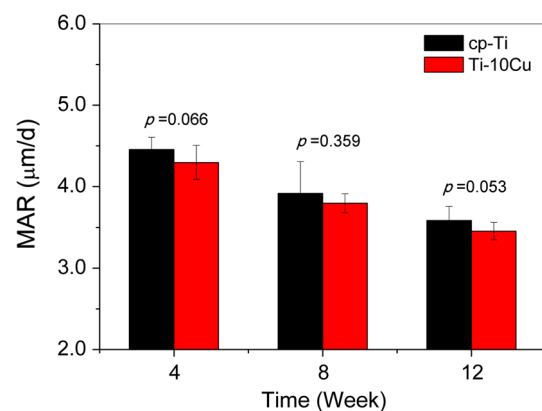


**Fig. 4** Mineral apposition rate (MAR) at different implantation durations. MAR decreased with the increase of the implantation duration, but no difference can be found between the cp-Ti group and the Ti-Cu group at all intervals ( $P > 0.05$ ) (Color figure online)

solution for 10–15 min. Then, the samples were transferred to aniline blue solution and stained for 5–10 min, rinsed briefly in distilled water and differentiated in 1 % acetic acid solution for 2–5 min and washed in distilled water, dehydrated very quickly through ethyl alcohol and clear in xylene. Finally, the samples, No 10–15, were mounted with

resinous mounting medium. The slice samples were observed with light microscope (Nikon eclipse 80i, Tokyo, Japan). Bone implant contact (BIC %) was calculated by superimposing the profile of the implant threads on the bone image from the actual implant site and counting the linear amount of bone that would be in contact with the

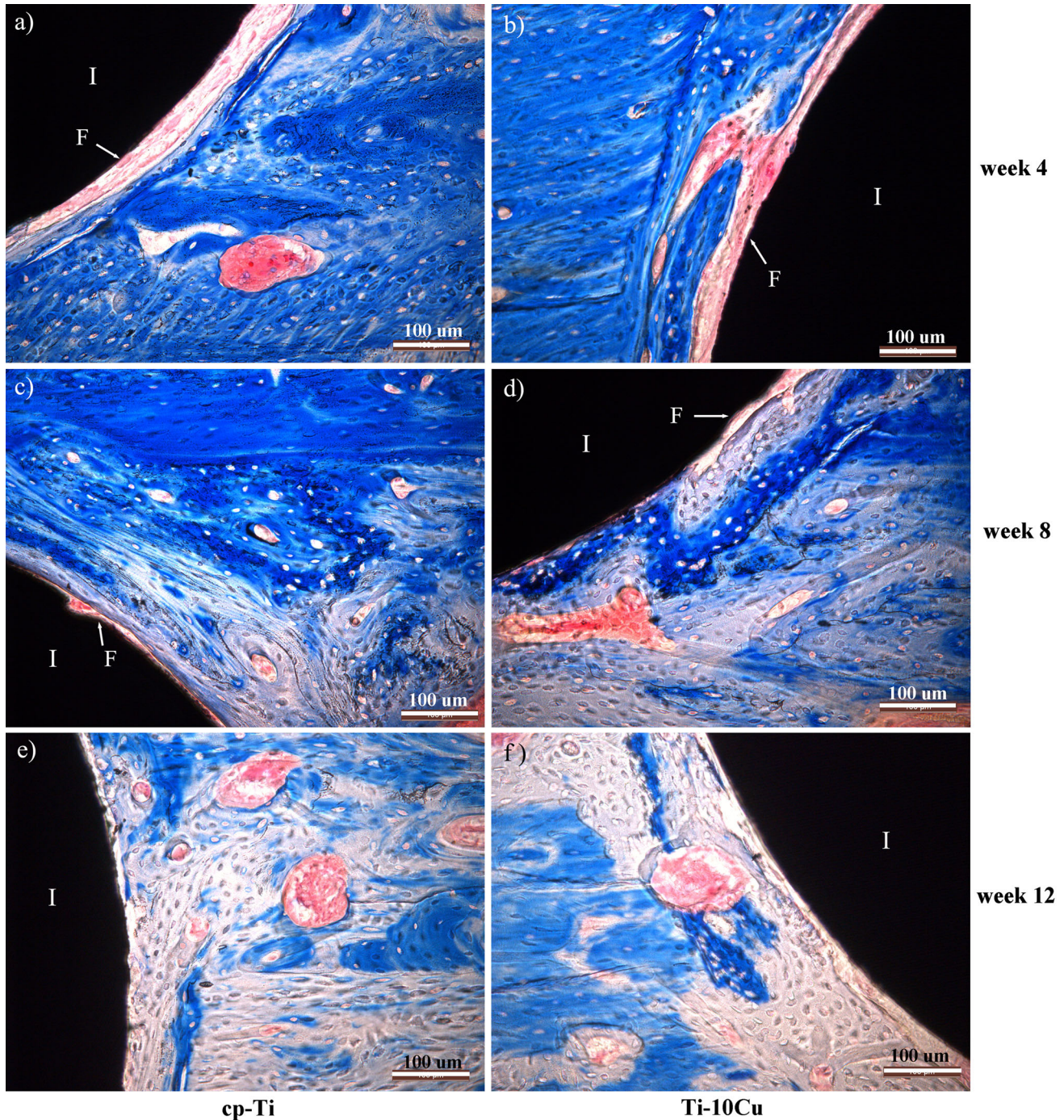


**Fig. 5** Pathological photographs of the bone/implant interfaces after 4 weeks, 8 weeks and 12 weeks postimplantation with Masson staining ( $\times 200$ ). Masson staining provides good distinction of osteoid, which was stained *blue-green*, from mature bone matrix,

which was stained *red*. **a, c, and e** cp-Ti implant, **b, d, and f** Ti-10Cu implant. **a, b** 4 weeks, **c, d** 8 weeks and **e, f** 12 weeks. (*I* implant; *F* fibroblast band) (Color figure online)



implant surface, which were measured on the screen by an image analysis software (Image-Pro Plus 6.0, USA). Parameter calibrations for magnification and image acquisition were fixed on the basis of standardized conditions imposed before the analysis.

## 2.7 Statistical analysis

Data were all expressed as mean  $\pm$  SD. Difference within group was analyzed by two-way ANOVA. Statistical significance was defined as  $P < 0.05$ .

## 3 Results

### 3.1 X-ray photo

Figure 2 shows the X-ray photos of the bone samples with cp-Ti implant and Ti-10Cu implant at 4, 8 and 12 weeks postimplantation. From the X-ray photos, no low density bone around implants was found. No difference in bone density was found between cp-Ti group and Ti-10Cu group at each time point.

### 3.2 Fluorescent microscopy

The fluoroscopic images of the cross-section of the bone samples with cp-Ti implant and Ti-10Cu implant after 4, 8, and 12 weeks implantation are shown in Fig. 3. Newly formed bone tissue was observed around the implant, as indicated by the green light circles. At week 4, there were obvious green light circles around implant in two groups and the gaps existed between the two green light circles, as shown in Fig. 3a and b. At week 8, as shown in Fig. 3c and d, the intensity of green light was weaker than that at week 4, indicating that the new bone formation was reduced. After 12 weeks implantation, as shown in Fig. 3e and f, little green light could be found around the implants, displaying that the new bone formation were nearly completed. No difference in the fluorescent microscopy was observed between cp-Ti group and Ti-10Cu group.

The new bone formation is expressed by MAR. Figure 4 shows the calculated MAR values at different implantation durations. For both cp-Ti group and Ti-10Cu group, MAR decreased significantly with the increasing of the implantation duration ( $P < 0.05$ ), indicating that the bone tissue grew fast at the beginning stage of the healing process. However, no difference in MAR value between cp-Ti group and Ti-10Cu group could be found at all investigated intervals ( $P > 0.05$ ), although MAR value of cp-Ti group was slightly higher than that of Ti-10Cu group.

### 3.3 Masson staining

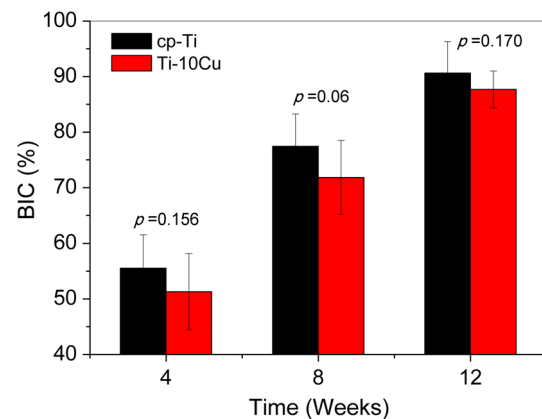
To confirm the bone compatibility of the cp-Ti and the Ti-10Cu implants, the quality of new-formed bone was further evaluated by Masson staining, as shown in Fig. 5. At week 4, fibrous connective tissue could be found at the bone/implant interface in the both groups. After 8 weeks, with diminishing fibrous tissue, more and more woven bone could be found around both cp-Ti and Ti-10Cu implant. Also new vascular formation and irregular osteocytes were found. At week 12, both cp-Ti and Ti-10Cu implants have been completely encapsulated by mature woven bone, which has more regular osteocytes and Harversian system.

Figure 6 shows BIC values of cp-Ti group and Ti-10Cu group at the bone/implant interface after different implantation durations. With the extension of the implantation, BIC increased significantly in both cp-Ti group and Ti-10Cu group ( $P < 0.05$ ). After 4 weeks postimplantation, nearly 50–55 % the implant surface was contacted with bone tissue. After 12 weeks postimplantation, up to 90 % the surface was contacted with new-formed mineralized bone. However, no difference could be found in BIC between cp-Ti group and Ti-10Cu group at all intervals although BIC values of cp-Ti group were slightly higher than that of Ti-10Cu group.

### 3.4 Immunohistochemistry

#### 3.4.1 BMP-2 expression

Immunohistochemistry staining was performed to evaluate the expressions of BMP-2 and TGF- $\beta$ 1, two established protein markers for osteogenesis, at the bone/implant interface. The amount of the two protein markers were represented by the intensity of the brown color.



**Fig. 6** Bone implant contact (BIC) at the bone/implant interfaces at different time points (Color figure online)

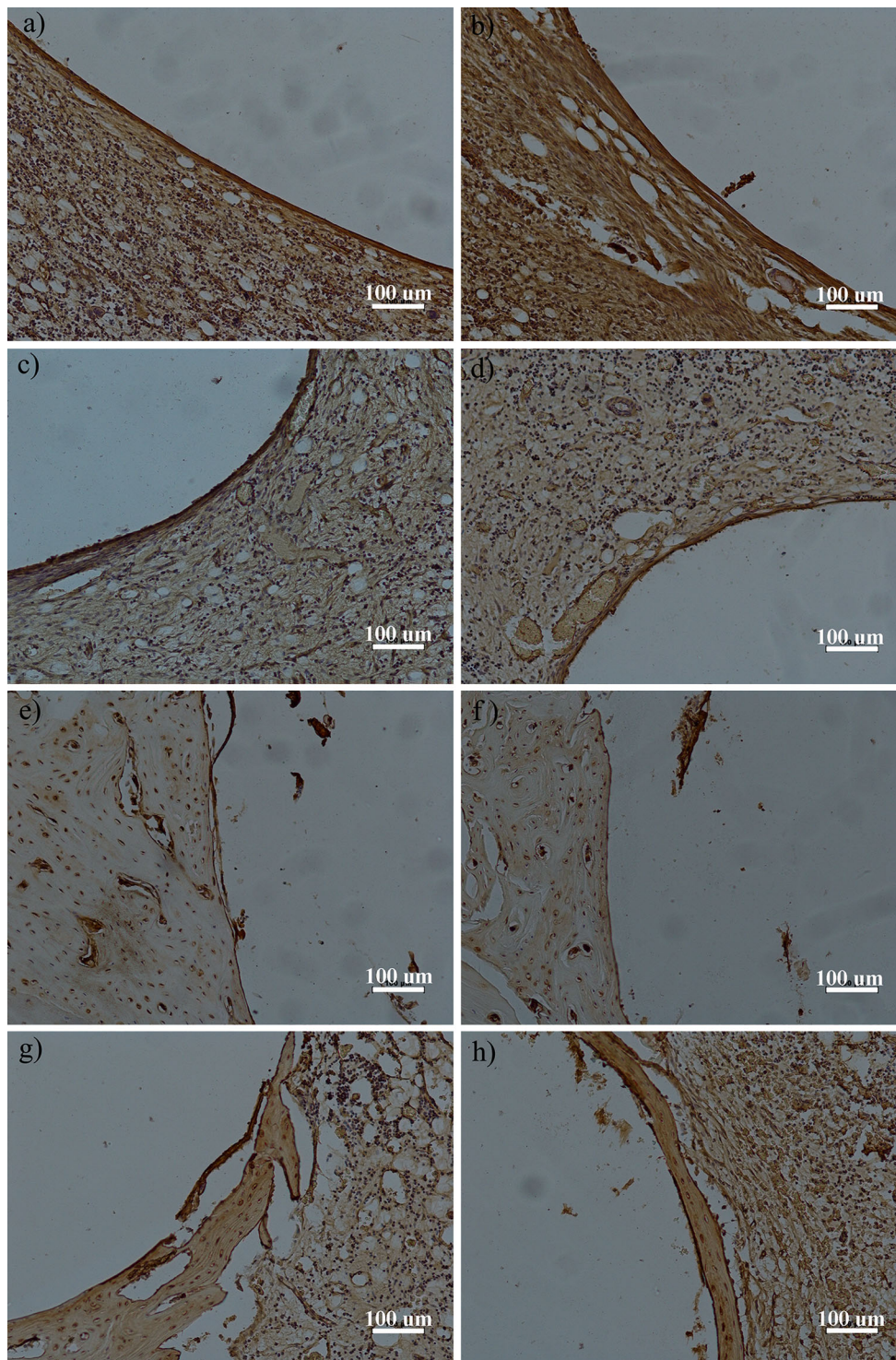


**Fig. 7** Photomicrographs of BMP-2 expression at the interfaces between the implants and the bone tissue after 1, 2, 3 and 4 weeks postimplantation ( $\times 200$ ). **a, c, e** and **g** samples with cp-Ti implant; **b,**

**d, f** and **h** samples with Ti-10Cu implants; **a, b** 1 week, **c, d** 2 weeks, **e, f** 3 weeks, **g, h** 4 weeks

Figure 7 shows BMP-2 staining photomicrograph at the bone/implant interface after different periods of implantation. Figure 8 shows MOD in BMP-2 expression at the

bone/implant interface after different periods of implantation. At week 1, strong positive activities were observed at the interfaces in both cp-Ti group and Ti-10Cu group, and



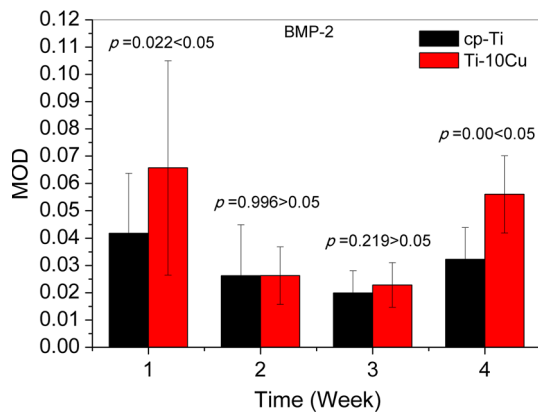


**Fig. 8** MOD values of BMP-2 expression at the interface between the implant and the bone tissue after different periods of implantation (Color figure online)

the MOD value in Ti-10Cu group was significantly higher than that in cp-Ti group ( $P < 0.05$ ). At week 2, the positive activities in both groups decreased significantly, but no difference was observed between the groups. At week 3, the positive activities decreased slight again, and no difference was observed between the groups. At week 4, the positive activities increased again significantly in comparison with the values at week 2 and 3, but significant difference was found between the groups ( $P < 0.05$ ).

### 3.4.2 TGF- $\beta$ 1 expression

Figure 9 shows TGF- $\beta$ 1 staining photomicrograph at the bone/implant interfaces after different periods of implantation. Figure 10 shows MOD in TGF- $\beta$ 1 expression at the bone/implant interface after different periods of implantation. A high TGF- $\beta$ 1 expression was observed at week 1 in both cp-Ti group and Ti-10Cu group. Then, MOD value decreased significantly at week 2, then increased at week 3 and week 4. However, no difference could be found in TGF- $\beta$ 1 expression between cp-Ti group and Ti-10Cu group at all implantation durations ( $P > 0.05$ ).

## 4 Discussion

Titanium alloys have been widely used as orthopedic implant materials and dental implants due to their good biocompatibility, good corrosion resistance and good mechanical properties. However, as stated in the introduction section, bacterial infection after implant placement is still a significant rising complication.

Previous studies on the antibacterial materials have demonstrated that the high antibacterial property is closely related to the  $\text{Cu}^{2+}$  ion release concentration from alloys

[17]. Copper is an essential trace element that is vital to the health of all living things (humans, plants, animals and microorganisms). However, like all essential elements and nutrients, too much or too little nutritional ingestion of copper can result in a corresponding condition of copper excess or deficiency in the body, each of which can lead to tissue injury and disease. World Health Organization (WHO) recommends the minimum acceptable intake of copper approximately 1.3 mg/day. Study has shown that the  $\text{Cu}^{2+}$  ion concentration released from Ti-10Cu was about 0.050 mg/L after 3 days immersion in 0.9 % NaCl solution in vitro [6], which is much lower than the recommended value. *In vivo* research has indicated that  $\text{Cu}^{2+}$  ion concentration in blood was about 52–53  $\mu\text{g}/\text{dl}$  (0.52–0.52 mg/L) during 14 days postimplantation and no difference was found before and after the implantation of Cu-containing steel [9].

On the other hand, the high  $\text{Cu}^{2+}$  ion concentration at the implantation site may bring about influence to the surrounding cells and tissues. In Li's research, Cu(II) ion was used to prepare Cu substituted hydroxyapatite [18]. The release of  $\text{Cu}^{2+}$  ion led to high antibacterial properties but also cytotoxicity to cell line HFOB 1.19 although the exact Cu ion concentration was not reported. Cortizo et al. [19] tested Cu toxicity to URM106 rat osteosarcoma and MC3T3E1 osteoblast cell lines. They observed 40–50 % decrease in surviving URM106 or MC3T3E1 cells at 104  $\mu\text{g}/\text{mL}$   $\text{Cu}^{2+}$  ion and all cells were dead by 48 h at 225  $\mu\text{g}/\text{mL}$ .

Studies on dental alloys showed a trend that copper and silver were the metal elements which induced cytotoxic effects of the alloys [20]. Strong tissue reactions were evoked after subcutaneous implantation of a Pd/Cu-alloy in guinea pigs [21]. In dogs, copper-based crowns released copper ion into the adjacent gingiva, which inflamed it [21]. But in this research, we have not found a reliable way to detect the  $\text{Cu}^{2+}$  ion concentration around the implants. Cp-Ti and Ti-10Cu were implanted into the body of rabbit femur to evaluate the influence of Ti-Cu alloy to the osseointegration. Other researchers used mechanical push out test to evaluate the osseointegration of the implants, which would yield more accurate data, and we would use this method in later experiments. Our previous study has confirmed that  $\text{Cu}^{2+}$  ion released from Ti-10Cu alloy did not cause cytotoxicity to MG63 and promoted ALP activity of MG63 [7]. Recently, Ren's results [4] indicated that some gene expressions of osteoblasts (MG3T3-E1), such as ALP, Col 1, OPN and Runx2, were all obviously increased for the Cu-containing 317L steel in comparison with 317L steel, indicating that  $\text{Cu}^{2+}$  ion released from Cu-containing 317L could promote the process of osteogenesis. All these results display that the bio-function of  $\text{Cu}^{2+}$  ion is strongly dependent on  $\text{Cu}^{2+}$  ion concentration. The balance

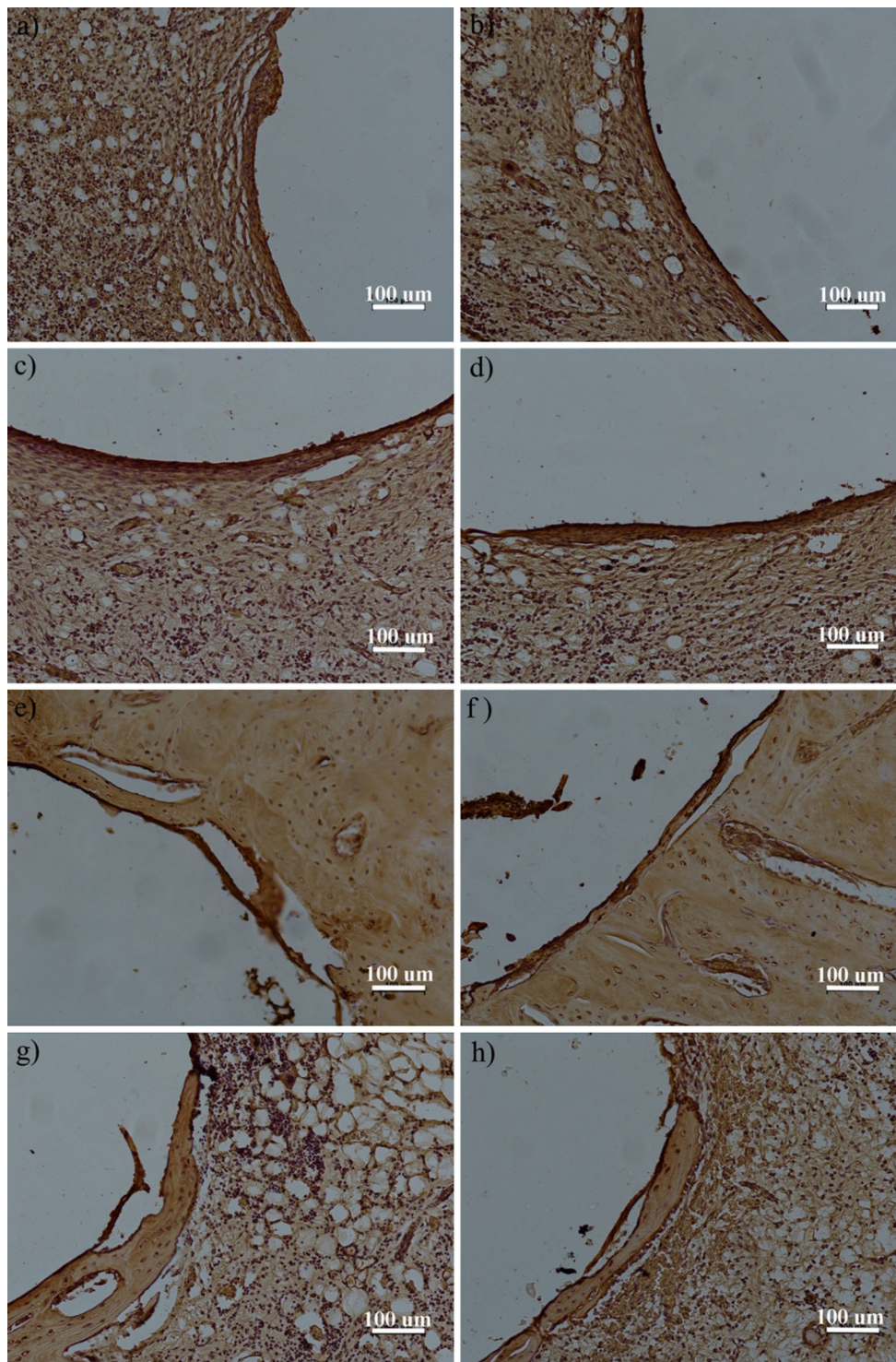


**Fig. 9** Photomicrographs of TGF- $\beta$ 1 expression at the interfaces between the implants and the bone tissue after 1, 2, 3 and 4 weeks postimplantation ( $\times 200$ ). **a, c, e** and **g** samples with cp-Ti implant; **b,**

**d, f** and **h** samples with Ti-10Cu implants; **a, b** 1 week, **c, d** 2 weeks, **e, f** 3 weeks, **g, h** 4 weeks

between the antibacterial property and biocompatibility will be very important for the development of Cu containing antibacterial material.

In this paper, X-ray photo, fluorescent observation and routine pathological examination clearly demonstrated that good bone tissue response to cp-Ti implant and Ti-10 Cu



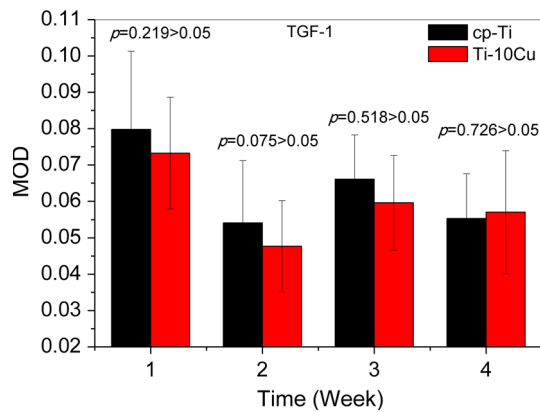


**Fig. 10** MOD values of TGF- $\beta$ 1 expression at the interface between the implant and the bone after different periods of implantation (Color figure online)

implant during up to 12 weeks implantation duration. However, although cp-Ti groups showed slightly higher MAR value and BIC value than Ti-10Cu group at the investigated intervals, no statistically significant difference can be found between these two groups: the Cu<sup>2+</sup> ion release neither promoted nor resisted bone response. This result was different from Ren's *in vivo* study [4], which confirmed the enhancement of early osteogenesis on the 317L-Cu steel in both higher amount of new bones and higher bonding force between the bone tissue and the steel implant.

Numerous growth factors have been implicated in the repair of fracture healing, so expressions of bone growth factors can be used to evaluate osteogenesis at the bone/implant interface. Among those growth factors, BMP-2 plays a crucial role in normal skeletal development as well as bone healing, and is able to activate transcription of genes involved in cellular migration, proliferation and differentiation [22]. It was reported that endogenous BMP-2 is an indispensable osteogenic stimulus for initiation of fracture healing in mice. In addition, it is believed that TGF- $\beta$ 1 stimulates osteogenesis, angiogenesis, fibroblast migration, and deposition of matrix and has osteoinductive properties [23, 24].

In the present studies, Ti-10Cu group showed a significantly higher BMP-2 expression at week 1 and week 4 than cp-Ti group. But no difference could be found in BMP-2 expression at week 2 and week 3 and in TGF- $\beta$ 1 expression at all intervals. No direct relationship between copper ion and the bone repair has been established [25], but copper has a close association and role in angiogenic process and is known to initiate endothelial cells toward angiogenesis [26–31]. BMP-2, a member of the morphogenetic proteins group and important mediator of osteoblast differentiation, is produced by the endothelium and smooth muscles of the vessels [32]. And it could induce

neovascularization by activating endothelial cells, or enhancing the synthesis of VEGF indirectly [33]. Dietrich [34] has proven that angiogenesis similarly went before osteosynthesis, regulated this process with the production of BMP-2 and served as a scaffold for osteoblasts during postnatal osteosynthesis in the mandible. These maybe the causes of the significantly higher BMP-2 expression and unchanged TGF- $\beta$ 1 expression in Ti-10Cu group, but we couldn't explain the decrease in BMP-2 expression at weeks 2 and 3 in both groups, which would be illustrated in the following experiment to clarify the relationship of VEGF and BMP-2. The values of MAR, which decreased with the increase of the implantation duration, indicated that bone tissue grew fast at the beginning of the healing process and slowed down by week 12, and this result was aligned with the expression of BIC %, which increased significantly in both groups with time. The mineral addition rate decreased but the amount of new-formed mineralized bone increased in both groups.

From the above results and discussion, the Cu<sup>2+</sup> ion released from Ti-10Cu implant did not delay bone healing. The stimulation of copper ion might benefit bone formation *in vivo*. Ti-10Cu alloy has good bone biocompatibility as cp-Ti, which brings no toxicity to the surrounding cell and tissue and no delay to bone healing. The good bone response of this alloy suggests that Ti-10Cu might be used in the dental and orthopedic implants. However, there is much research work to be done to assess the application possibility.

## 5 Conclusion

There was significantly increased BMP-2 expression in Ti-10Cu group at 1 and 4 weeks, and no difference in MAR, BIC and TGF- $\beta$ 1 expression has been detected between cp-Ti group and Ti-10Cu group. Ti-10Cu sintered alloy exhibited as good bone biocompatibility as cp-Ti *in vivo*.

**Acknowledgments** The authors would like to acknowledge the financial support from National Natural Science Foundation (81071262, 31271024, 31470930), Foundation for Key Program of Ministry of Education, China (313014), and Funding from Northeastern University (985 program and N141008001, LZ2014018), China.

## References

- Gristina AG, Oga M, Webb LX, Hobgood CD. Adherent bacterial colonization in the pathogenesis of osteomyelitis. *Science*. 1985;228:990–3.
- Costerton JW, Lewandowski Z, Caldwell DE, Korber DR, Lappin-Scott HM. Microbial biofilms. *Annu Rev Microbiol*. 1995;49:711.

3. Green SA. Complications of external skeletal fixation. *Clin Orthop Relat Res.* 1983;180:109–16.
4. Ren L, Yang K, Guo L, Chai H. Preliminary study of anti-infective function of a copper-bearing stainless steel. *Mater Sci Eng C.* 2012;32:1204–9.
5. Shirai T, Tsuchiya H, Shimizu T, Ohtani K, Zen Y, Tomita K. Prevention of pin tract infection with titanium–copper alloys. *J Biomed Mater Res Part B.* 2009;91B:373–80.
6. Zhang E, Li F, Wang H, Liu J, Wang C, Li M, et al. A new antibacterial titanium–copper sintered alloy: preparation and antibacterial property. *Mater Sci Eng C.* 2013;33:4280–7.
7. Liu J, Zhang X, Wang H, Li F, Li M, Yang K, et al. The antibacterial properties and biocompatibility of a Ti–Cu sintered alloy for biomedical application. *Biomed Mater.* 2014;9:025013.
8. Liu J, Li F, Liu C, Wang H, Ren B, Yang K, et al. Effect of Cu content on the antibacterial activity of titanium–copper sintered alloys. *Mater Sci Eng C.* 2014;35:392–400.
9. Chai H, Guo L, Wang X, Fu Y, Guan J, Tan L, et al. Antibacterial effect of 317L stainless steel contained copper in prevention of implant-related infection in vitro and in vivo. *J Mater Sci Mater Med.* 2011;22:2525–35.
10. Hong IT, Koo CH. Antibacterial properties, corrosion resistance and mechanical properties of Cu-modified SUS 304 stainless steel. *Mater Sci Eng A.* 2005;393:213–22.
11. Jeyachandran YL, Venkatachalam S, Karunagarana B. Bacterial adhesion studies on titanium, titanium nitride and modified hydroxyapatite thin films. *Mater Sci Eng C.* 2007;27:35–41.
12. Amalric J, Mutin PH, Guerrero G. Phosphonate monolayers functionalized by silver thiolate species as antibacterial nanocoatings on titanium and stainless steel. *J Mater Chem.* 2009;19:141–9.
13. Tian Y, Cao H, Qiao Y, Meng F, Liu X. Antibacterial activity and cytocompatibility of titanium oxide coating modified by iron ion implantation. *Acta Biomater.* 2014;10:4505–17.
14. Fang J, Zhao JH, Sun Y, Ma HY, Yu XL, Ma Y, et al. Biocompatibility and antibacterial properties of zinc-ion implantation on titanium. *J Hard Tissue Biol.* 2014;23:35–43.
15. Wan YZ, Xiong GY, Liang H, Raman S, He F, Huang Y. Modification of medical metals by ion implantation of copper. *Appl Surf Sci.* 2007;253:9426–9.
16. Faúndez G, Troncoso M, Navarrete P, Figueroa G. Antimicrobial activity of copper surfaces against suspensions of *Salmonella enterica* and *Campylobacter jejuni*. *BMC Microbiology.* 2004;. doi:10.1186/1471-2180-4-19.
17. Derynck R, Zhang Y. Intracellular signalling: the mad way to do it. *Curr Biol.* 1996;6:1226–9.
18. Li Y, Ho J, Ooi CP. Antibacterial efficacy and cytotoxicity studies of copper (II) and titanium (IV) substituted hydroxyapatite nanoparticles. *Mater Sci Eng C.* 2010;30:1137–44.
19. Cortizo MC, De Mele MA, Cortizo AM. Metallic dental material biocompatibility in osteoblastlike cells correlation with metal ion release. *Biol Trace Elem Res.* 2004;100:151–68.
20. Schmalz G, Garhammer P. Biological interactions of dental cast alloys with oral tissues. *Dent Mater.* 2002;18:396–406.
21. Yang L, Perez-Amodio S, Barrère-de Groot FYF, Everts V, van Blitterswijk CA, Habibovic P. The effects of inorganic additives to calcium phosphate on in vitro behavior of osteoblasts and osteoclasts. *Biomaterials.* 2010;31:2976–89.
22. Thurman RB, Gerba CP. The molecular mechanisms of copper and silver ion disinfection of bacteria and viruses. *CRC Crit Rev Environ Control.* 1989;18:295–315.
23. Noda M. In vivo stimulation of bone formation by transforming growth factor. *Endocrinology.* 1989;124:2991–4.
24. Zhang H, Ahmad M, Gronowicz G. Effects of transforming growth factor-beta 1(TGF-b1) on in vitro mineralization of human osteoblasts on implant materials. *Biomaterials.* 2003;24:2013–20.
25. Habibovic P, Barralet JE. Bioinorganics and biomaterials: bone repair. *Acta Biomater.* 2011;7:3013–26.
26. Hu GF. Copper stimulates proliferation of human endothelial cells under culture. *J Cell Biochem.* 1998;69:326–35.
27. Gerard C, Bordeleau L-J, Barralet J, Doillon CJ. The stimulation of angiogenesis and collagen deposition by copper. *Biomaterials.* 2010;31:824–31.
28. Harris ED. A requirement for copper in angiogenesis. *Nutr Rev.* 2004;62:60–4.
29. Lakhkar NJ, Lee I-H, Kim H-W, Salih V, Wall IB, Knowles JC. Bone formation controlled by biologically relevant inorganic ions: role and controlled delivery from phosphate-based glasses. *Adv Drug Deliv Rev.* 2013;65:405–20.
30. Raju KS, Alessandri G, Ziche M, Gullino PM. Ceruloplasmin, copper ions and angiogenesis. *J Natl Cancer Inst.* 1982;69:1183–8.
31. McAuslan BR, Reilly WG, Hannan GN, Gole GA. Angiogenic factors and their assay: activity of formyl methionyl leucyl phenylalanine, adenosine diphosphate, heparin, copper, and bovine endothelium stimulating factor. *Microvasc Res.* 1983;26:323–38.
32. Matsubara H, Hogan DE, Morgan EF, Mortlock DP, Einhorn TA, Gerstenfeld LC. Vascular tissues are a primary source of BMP2 expression during bone formation induced by distraction osteogenesis. *Bone.* 2012;51:168–80.
33. Langenfeld EM, Langenfeld J. Bone morphogenetic protein-2 stimulates angiogenesis in developing tumors. *Mol Cancer Res.* 2004;2:141–9.
34. Dietrich EM, Antoniades K. Bone–vasculature interactions in the mandible: is bone an angiogenic tissue? *Med Hypotheses.* 2012;79:582–4.